Article

Journal of
Nanoscience and Nanotechnology
Vol. 21, 2681–2686, 2021
www.aspbs.com/jnn



# Influence of Excess Potassium on Structural and Ferroelectric Properties of Lead-Free $Bi_{0.5}K_{0.5}TiO_3$ Thin Films

Nguyen Ngoc Minh[1], Bui Van Dan[1], Nguyen Duc Minh[3, 4], Guus Rijnders[4], and Ngo Duc Quan[2, 3, *]

[1] *Electrical and Electronic Faculty, Hung Yen University of Technology and Education, Hung Yen Province 160000, Vietnam*
[2] *School of Engineering Physics, Hanoi University of Science and Technology, Hanoi 100000, Vietnam*
[3] *International Training Institute for Materials Science (ITIMS), Hanoi University of Science and Technology, Hanoi 100000, Vietnam*
[4] *MESA+ Institute for Nanotechnology, University of Twente, 7500, AE, Enschede, The Netherlands*

Lead-free $Bi_{0.5}K_{0.5}TiO_3$ (BKT) ferroelectric films were synthesized on $Pt/Ti/SiO_2/Si$ substrates via the chemical solution deposition. The influence of the excess potassium on the microstructures and the ferroelectric properties of the films was investigated in detail. The results showed that the BKT films have reached the well-crystallized state in the single-phase perovskite structure with 20 mol.% excess amount of potassium. For this film, the ferroelectric properties of the films were significantly enhanced. The remnant polarization ($P_r$) and maximum polarization ($P_m$) reached the highest values of 9.4 $\mu C/cm^2$ and 32.2 $\mu C/cm^2$, respectively, under the electric field of 400 kV/cm.

**Keywords:** Lead-Free, Ferroelectric, Sol–Gel, BKT, Films.



## 1. INTRODUCTION

Solid solutions of $Bi_{0.5}K_{0.5}TiO_3$ (BKT) with other perovskites has the possibility to substitute for Pb(Zr, Ti)$O_3$ (PZT)-based materials in some practical applications. Being a perovskite with tetragonal symmetry at room temperature, BKT is a typical ferroelectric material possessing a relatively high Curie temperature, $T_c$, of 380 °C [1]. By XRD (X-ray diffraction) analysis, Ivanova et al. observed that the lattice parameters $a$ and $c$ of BKT materials are 0.3913 nm and 0.3993 nm, respectively [2]. The previous reports believed that BKT materials, mixed bismuth and alkali $A$-cations are candidates as a lead-free ferroelectric material with a large spontaneous polarization [3–5]. The key properties of BKT-based materials, such as ferroelectric properties, $d_{33}$ piezoelectric coefficient, energy storage density at the morphotropic phase boundary (MPB) need to be improved. In order to enhance the nature of this material, the origin and mechanism of its characteristics need to clearly identify. The recent experimental work [6] showed that the $Fe^{3+}$ ions substitution at Ti-site caused room temperature ferromagnetism and a reduction of bandgap in BKT materials. In addition, when substituted by other ions, such as $Mn^{2+}$ [7], $Ni^{2+}$ [8], or $Co^{2+}$ [9], BKT materials also revealed the room temperature ferromagnetism. Besides, the room temperature magnetic behaviors were also observed in the solid solution of BKT with $BiFeO_3$ (BFO) [10]. Zuo et al. observed strong enhancement of the magnetization and Curie temperature in solid solution between BKT and Co-modified BFO [11]. The room temperature ferromagnetic behaviors observed in BKT materials were attributed to: *i*/the mixed-valence states of ions [6, 7]; *ii*/the spin-exchange splitting between spin subbands induced by the presence of substitution ions and high-spin crystal field energy spectrum [9].

However, $K^+$ ion similar to $Bi^{3+}$ and $Na^+$ metal ions in $Bi_{0.5}Na_{0.5}TiO_3$-based ceramics (BNT) is believed to be likely volatile during fabrication. In addition, the starting materials such as $K_2CO_3$, $Na_2CO_3$, and $Bi_2O_3$ employed in preparing BKT, and BNT ceramics likely absorb moisture in the air, also cause a mass loss. To compensate for the loss of metal ions in the fabricating process, excess amounts of the initial chemicals are added. Recently, only a few studies referring to effects of Bi and/or Na nonstoichiometry have been reported [12–14]. Sung et al. [15] studied the effects of Na excess and defect on the structure and electrical properties of BNT ceramics. Structural

*Author to whom correspondence should be addressed.

distortion has been discovered and is a key factor affecting the piezoelectric coefficient ($d_{33}$) and the depolarization temperature ($T_d$). This is the origin of the inverse relationship between $d_{33}$ and $T_d$ or Curie temperature, $T_c$. Structural distortion is also occurred in the solid solution between BNT and $BaTiO_3$ and found to influence on $d_{33}$ and $T_d$ [16]. This factor contributes to another way to explain how the piezoelectric and ferroelectric properties are improved around the MPB, apart from the traditional one of the multi-phase coexistence [17].

In previous works, the influence of the processing conditions, such as the film thickness, annealing temperature and crystallization time on the electric properties of BKT-based films [18–21], were investigated. Via modifying *A* or *B*-site in the perovskite structure, we have enhanced significantly the electric properties of BKT-based films [22–25]. In this study, the effect of *K* excess on the microstructure and some properties of BKT films were investigated; Based on these results, we determined the optimal *K*-added concentration for the preparation, aiming to enhance the microstructure and piezo/ferroelectric properties of the BKT films.

## 2. EXPERIMENTAL DETAILS

BKT films were synthesized on $Pt/Ti/SiO_2/Si$-(100) substrates by chemical solution deposition (CSD). Potassium nitrate ($KNO_3$), bismuth nitrate [$Bi(NO_3)_3 \cdot 5H_2O$], and tetrabutyl titanium [$Ti\text{-}(OC_4H_9)_4$] were used as starting materials to prepare BKT precursor solution with the concentration of 0.30 M. Acetic acid ($CH_3COO\text{-}H$) and 2-ethoxyethanol ($CH_3OCH_2CH_2OH$) were chosen as cosolvent. During preparation, tetrabutyl titanium was dissolved in acetylace-tone ($CH_3COCH_2\text{-}COCH_3$) to prevent hydrolysis of tetrabutyl titanium caused by moisture in the air. Afterward, excess amounts of potassium nitrate were added to compensate for possible loss during high-temperature annealing. The mixture was constantly stirred for about 24 h until a transparent and stable yellow precursor solution was obtained. Each layer of BKT film was formed by spin coating precursor solution on $Pt/Ti/SiO_2/Si$ substrate at 4000 rpm for 30 s, drying at 150 °C for 5 min, and pyrolyzing at 450 °C for 5 min. This process was repeated until the BKT film obtained the desired thickness. Thermal annealing was conducted at 700 °C for 60 min to form ferroelectric phase in the BKT films.

Phase identification and crystalline orientation determination for the BKT films were carried out by X-ray diffraction analysis. The surface morphology and grain size of the films were investigated by field-emission scanning electron microscopy (FESEM). Square Pt top electrodes with various dimensions of 100 $\mu$m were formed via a lift-off technique to measure the ferroelectric properties. Polarization–electric field (*P–E*) hysteresis loops were determined using a TF Analyzer 2000 ferroelectric tester (aixACCT Systems GmbH, Germany) under various applied voltages ranging from −25 V to 25 V. All measurements were performed at room temperature.

## 3. RESULTS AND DISCUSSION

Surface morphology of BKT films was determined through FE-SEM and AFM images. Figure 1 illustrates 2 and 3-dimensional AFM images of BKT films with a scanning area of $40 \times 40$ $\mu m^2$. AFM images show that the surface of BKT films is relatively smooth and continuous. The surface roughness of the films is evaluated through the root-mean-square value (*RQ*) being in the range of 7 nm to 14 nm (Table I). Especially, when *K* excess concentration increases from 10% mol to 40% mol, the *RQ* value decreases.

Figure 2 illustrates the surface FE-SEM images of BKT films with *K* excess concentration of (a) 10, (b) 20, (c) 30 and (d) 40% mol. With explicit grain boundaries, the films show the well-defined grain morphology and the grains are uniformly distributed over the entire surface. It is observed



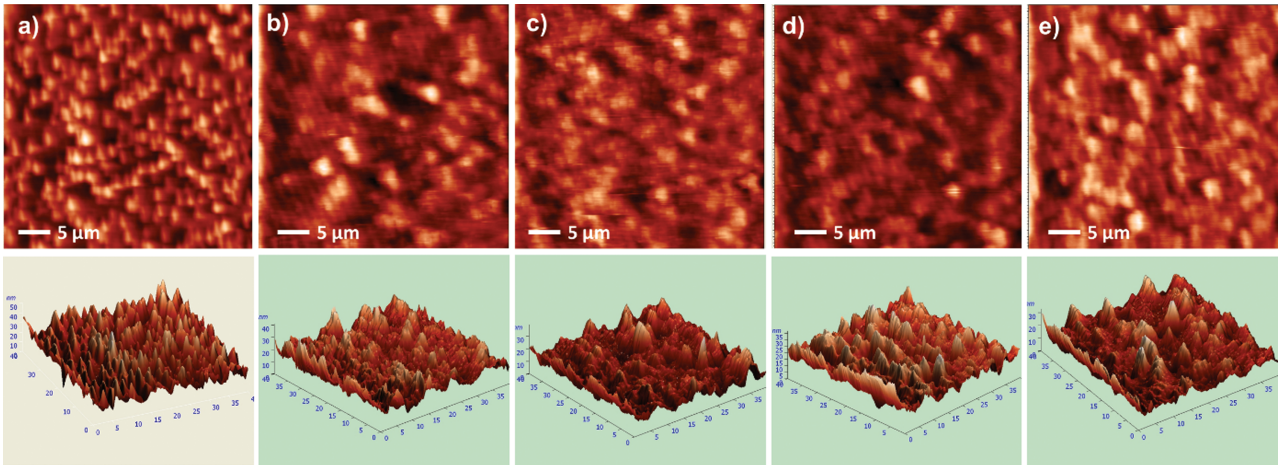


**Figure 1.** 2D–3D AFM images of BKT films with different *K* excess concentrations: (a) 0% mol, (b) 10% mol, (c) 20% mol, (d) 30% mol, (e) 40% mol.

**Table I.** The values of $RQ$, $P_m$, $P_r$, and $E_C$ as a function of $K$-excess concentration.

| $K$-excess content (%mol) | 00 | 10 | 20 | 30 | 40 |
|---|---|---|---|---|---|
| $RQ$ (nm) | 14 | 10 | 8 | 7 | 9 |
| $E_c$ (kV/cm) | 80 | 77 | 102 | 86 | 65 |
| $P_m$ ($\mu$C/cm$^2$) | 18.5 | 21 | 27.1 | 23.0 | 15.8 |
| $P_r$ ($\mu$C/cm$^2$) | 4.2 | 5.1 | 9.6 | 5.3 | 2.7 |

that $K$ excess content effects little the surface morphology of films. There are no cracks observed, but the number of small holes appears in the film surfaces. The formation of holes is attributed to the rapid removal of organic roots during high-temperature annealing. The evaporation of $K^+$ ions during the high-temperature annealing may also contribute to the formation of holes.

The films after a fabrication were analyzed by XRD. Figure 3(a) illustrates the XRD patterns of BKT films with $K$-excess concentration $x$ as 10, 20, 30 and 40% mol, respectively, with the $2\theta$ range of 25°–75°. All the patterns exhibit sharp diffraction peaks with crystal orientations (110), (200), (211) and (220) at $2\theta$ diffraction angles 31.7°, 47.8°, 59.4°, and 71.0°, respectively. These peaks characterize the perovskite structure with the tetragonal symmetry [12, 17]. Particularly, the peak (111) at the diffraction angle of 40° has an outstanding intensity comparing to other peaks defined by the Pt substrate. In the investigated $K$-excess range, no peaks of any strange phase are observed.

The XRD patterns of the films with a diffraction angle of $2\theta$ from 30.5° to 32.0° and from 47° to 48° are illustrated in Figure 3(b) respectively. The results show that the peak (200) has the superior intensity considered as the preferred orientation of the BKT films. The intensity value of the peak (200) varies corresponding to the rise of $K$-excess concentration. Figure 3(b) shows the dependence of the intensity peaks (110) and (200) on $K$-excess concentration. Peak intensity (110) tends to increase with $K$-excess concentration and reach the highest value at $K$-excess concentration of 20% mol. The peak (200) follows a different trend comparing to the peak (110). With the $K$-excess concentration of 10% mol, peak intensity (200) has the lowest value. Its value increases in proportion to the increase of $K$-excess concentration and reaches the maximum value at the $K$-excess concentration of 30% mol. However, when $K$-excess concentration increases to 40% mol, peak intensity (200) is reduced. The intensity of peaks (110) and (200) possess the low values at small $K$-excess concentration (0 and 10% mol) indicates that these films have a poor crystallinity. This is stemmed from the possible loss of $K^+$ ions during high-temperature annealing. And the amount of $K$ excess is not enough to compensate for the evaporated metal ion content, forming $A$-site defects. With $K$-excess concentration of 30% mol, peak intensity (200) reaches the highest value, as a result of the $K^+$ ion content evaporated during crystallization has been completely compensated.

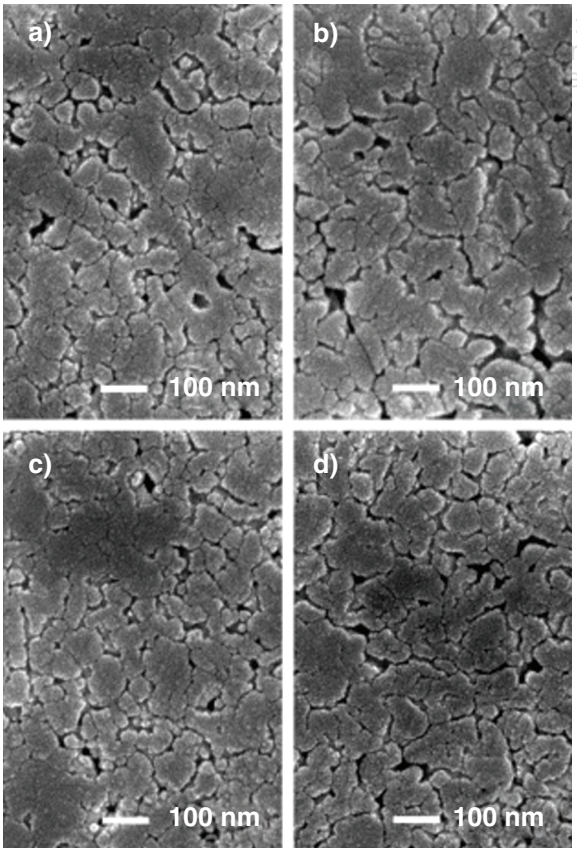


**Figure 2.** FE-SEM images of BKT films with different $K$ excess concentrations: (a) 10% mol, (b) 20% mol, (c) 30% mol, (d) 40% mol.

Figure 4(a) illustrates the polarization ($P$–$E$) hysteresis loops of BKT films with $K$-excess concentration of 10, 20, 30 and 40% mol. All the BKT films show the polarization ($P$–$E$) hysteresis loops with the typical shape of ferroelectric materials. Figure 4(b) illustrates the dependence of $P_m$, $P_r$, and $E_c$ values on $K$-excess concentration. The pure BKT film with $K$-excess concentration of 0% mol exhibits relatively low $P_m$ and $P_r$ values, respectively 18.5 $\mu$C/cm$^2$ and 4.2 $\mu$C/cm$^2$, while its $E_c$ coercive field is quite high, about 80 kV/cm. $P_m$ and $P_r$ are significantly enhanced when $K$-excess concentration is increased. Both of these parameters reach their maximum values ($P_m = 27.1$ $\mu$C/cm$^2$ and $P_r = 9.6$ $\mu$C/cm$^2$) at the $K$-excess content of 20% mol. When $K$-excess concentration increases to 40% mol, $P_m$ and $P_r$ decreased to the values of 15.8 $\mu$C/cm$^2$ and 2.7 $\mu$C/cm$^2$, respectively. The coercive field $E_c$ has a changing trend similar to $P_m$ and $P_r$. $E_c$ also rises with an increase of $K$-excess concentration and reaches the maximum value of about 102 kV/cm

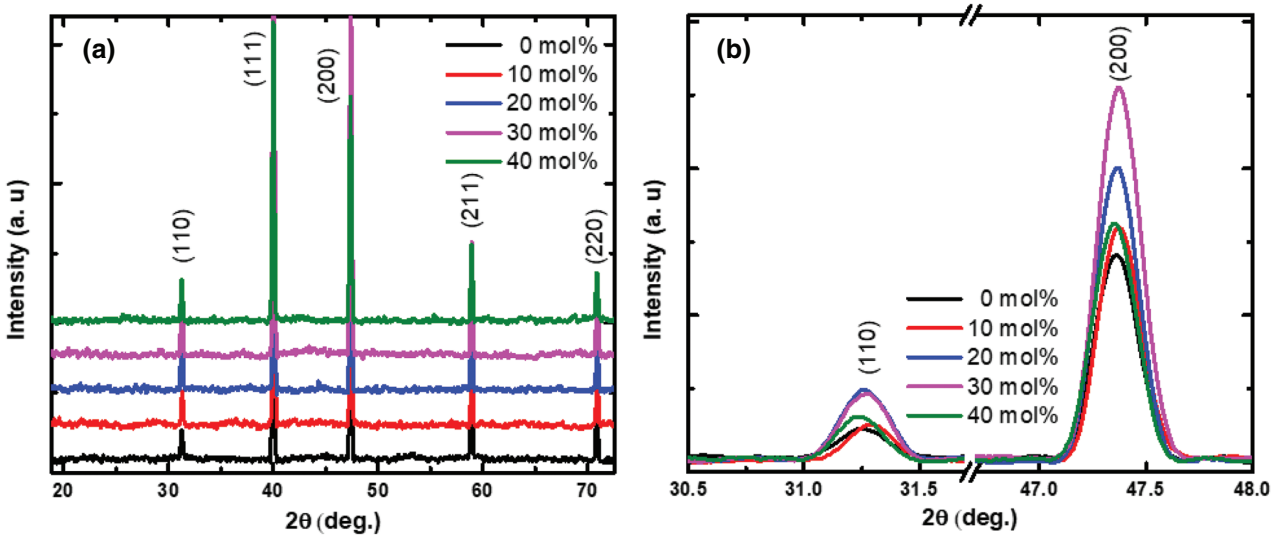


**Figure 3.** X-ray diffraction patterns of BKT films in the $2\theta$ ranges of 25°–75°, and (b) X-ray diffraction patterns in the $2\theta$ ranges of 30.5°–32.0° and 47°–48°.

at 20% mol *K*-excess concentration. With low *K*-excess concentration, the amount of *K* excess is not enough to compensate for the evaporation of metal ions during high-temperature annealing, forming defects at *A*-site and oxygen vacancies. Chemically, Bi and K deficiency can be described as follows:

$$Bi_{loss} \longrightarrow 2V'''_{Bi} + 3V^{\cdot\cdot}_{O} \quad (1)$$

$$K_{loss} \longrightarrow 2V'_{K} + V^{\cdot\cdot}_{O} \quad (2)$$



For *K* deficiency, a matrix of defect complexes ($V'_K - V^{\cdot\cdot}_O - V'_K$) is formed by $V'_{Bi}$ and $V^{\cdot\cdot}_O$. For K deficiency, a matrix of defect complexes ($V'_K - V^{\cdot\cdot}_O - V'_K$) is proposed to explain the experimental results of ferro/piezoelectric properties [15]. It is believed that oxygen vacancies ($V^{\cdot\cdot}_O$) cause a pinning effect on the domain walls, which reduces the mobility of the domain walls [26, 27]. This causes a high coercive field $E_c$, while decreases maximum polarization $P_m$ and remnant polarization $P_r$. However, the grain boundary pinning effect caused by the defect complexes ($V'_K - V^{\cdot\cdot}_O - V'_K$) appears, reducing the grain size. When the *K*-excess concentration is increased to 20% mol, the evaporated $K^+$ ions are completely supplemented, leading to the defect complex $V'_K - V^{\cdot\cdot}_O - V'_K$ vanishing. The domain wall pinning effect is suppressed, followed by a decrease of $E_c$ to the minimum value. The domains become more flexible, as a result, $P_r$ and $P_m$ increase to their maximum values. For Bi nonstoichiometry, a matrix of the defect complexes is formed by $V'_{Bi}$ and $V^{\cdot\cdot}_O$ is $2(V'_K - V^{\cdot\cdot}_O)' - V^{\cdot\cdot}_O$. These defect complexes need a combination of five defects, which rarely occurs. So, oxygen vacancies $V^{\cdot\cdot}_O$ will be released and become more flexible to pin the domain walls [28]. In other words, there are defects $V^{\cdot\cdot}_O$ for pinning the domain walls but no defect complexes for

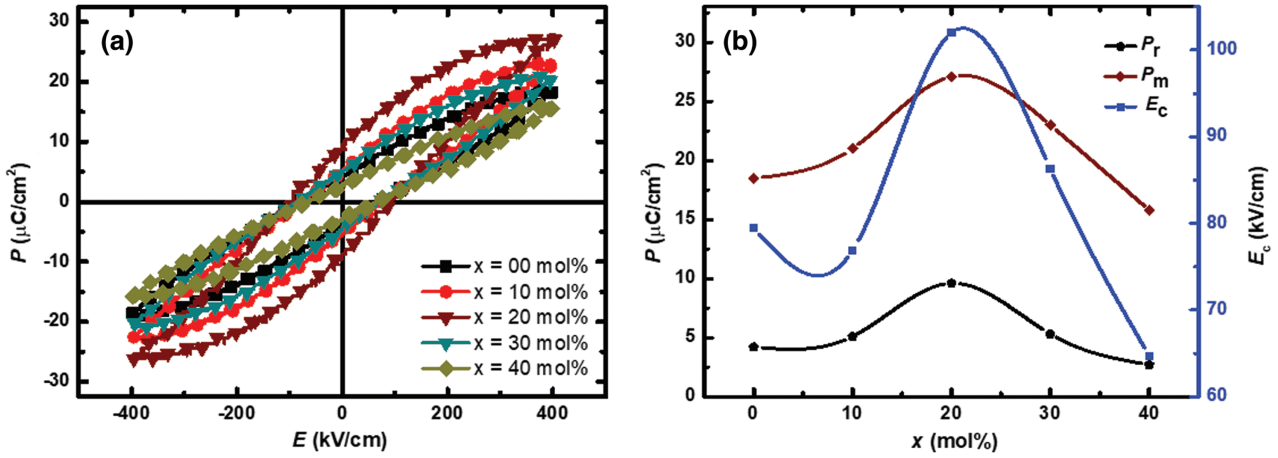


**Figure 4.** (a) *P*–*E* ferroelectric hysteresis loops, (b) the dependence of $P_m$, $P_r$, and $E_c$ of BKT films on *K*-excess concentration with the electric field of 400 kV/cm.

pinning the grain boundaries, leading to the decrease of $P_r$ and $P_m$ values in the BKT films at $K$-excess concentration of 40% mol, as illustrated in Figure 4(b). The loss of $Bi^{3+}$ ions during treatment is similar to the loss of $Pb^{2+}$ in PZT material [29]. As shown as XRD results (Fig. 3(b)), the films with the $K$-excess content of 30% mol possess the best crystallization, but their ferroelectric properties lower than those of films added 20% mol potassium. For the $K$-excess contents up to 30% mol, the $K$-added amount surpasses the evaporated content, forming a small amount of metal oxide $K_2O$. This metal oxide causes an increase in leakage current, decreasing the ferroelectric behavior of the films.

## 4. CONCLUSION

With the spin-coating routine, BKT films were successfully synthesized on Pt/Ti/$SiO_2$/Si substrates. The effect of $K$ excess on the structure and electrical properties of films were examined in detail. The results showed that $K$-excess concentration significantly influences the microstructure and ferroelectric properties of BKT films. The optimal $K$-excess concentration is 20% mol, where the BKT films are well-crystallized with a single perovskite phase component. The ferroelectric properties of these films are significantly enhanced compared to other films. Both $P_r$ and $P_m$ reach the highest values of 9.6 $\mu C/cm^2$ and 27.1 $\mu C/cm^2$ at the electric field of 400 kV/cm. The improvement of ferroelectric properties of BKT films at $K$-excess concentration of 20% mol is due to the amount of $K$ excess compensated completely for the loss of $K^+$ ions during treatment. The number of oxygen vacancies pinning domain wall decrease followed by an improvement in the polarization of the films.

**Acknowledgment:** This research was supported by Nippon Glass Sheet Foundation and Hung Yen University of Technology and Education under grant number UTEHY.L.2020.03.

## References and Notes

1. Buhrer, C.F., **1962**. Some properties of bismuth perovskites. *Journal of the Chemical Society*, *36*(3), pp.798–803.
2. Ivanova, V.V., Kapyshev, A.G., Venevtsev, Y.N. and Zhdanov, G.S., **1962**. X-ray determination of the symmetry of elementary cells of the ferroelectric materials $(K_{0.5}Bi_{0.5})TiO_3$ and $(Na_{0.5}Bi_{0.5})TiO_3$ and of high-temperature phase transitions in $(K_{0.5}Bi_{0.5})$ $TiO_3$. *Izvestiya Akademii Nauk SSSR. Seriya Matematicheskaya, 26*(2), pp.354–356.
3. Hiruma, Y., Aoyagi, R., Nagata, H. and Takenaka, T., **2005**. Ferroelectric and piezoelectric properties of $(Bi_{1/2}K_{1/2})TiO_3$ Ceramics. *Japanese Journal of Applied Physics*, *44*(7A), pp.5040–5044.
4. Li, Z.F., Wang, C.L., Zhong, W.L., Li, J.C. and Zhao, M.L., **2003**. Dielectric relaxor properties of $K_{0.5}Bi_{0.5}TiO_3$ ferroelectrics prepared by sol–gel method. *Journal of Applied Physics*, *94*(4), pp.2548–2552.
5. Yang, J., Hou, Y., Wang, C., Zhu, M. and Yan, H., **2007**. Relaxor behavior of $(K_{0.5}Bi_{0.5})TiO_3$ ceramics derived from molten salt synthesized single-crystalline nanowires. *Applied Physics Letters*, *91*(2), Article ID: 023118.
6. Dung, D.D., Thiet, D.V., Odkhuu, D., Cuong, L.V., Tuan, N.H. and Cho, S., **2015**. Room-temperature ferromagnetism in Fe-doped wide band gap ferroelectric $Bi_{0.5}K_{0.5}TiO_3$ nanocrystals. *Materials Letters*, *156*, pp.129–133.
7. Tuan, N.H., Thiet, D.V., Odkhuu, D., Bac, L.H., Binh, P.V. and Dung, D.D., **2017**. Defect induced room temperature ferromagnetism in lead-free ferroelectric $Bi_{0.5}K_{0.5}TiO_3$ materials. *Physica B: Condensed Matter*, *532*, pp.108–114.
8. Dung, D.D., Dung, N.Q., Doan, N.B., Linh, N.H., Bac, L.H., Trung, N.N., Duc, N.V., Thanh, L.T.H., Cuong, L.V., Thiet, D.V. and Cho, S., **2020**. Defect-mediated room temperature ferromagnetism in lead-free ferroelectric $Na_{0.5}Bi_{0.5}TiO_3$. *Journal of Superconductivity and Novel Magnetism*, *33*(4), pp.911–920.
9. Cuong, L.V., Tuan, N.H., Odkhuu, D., Van Thiet, D., Dung, N.H., Bac, L.H. and Dung, D.D., **2017**. Observation of room-temperature ferromagnetism in Co-doped $Bi_{0.5}K_{0.5}TiO_3$ materials. *Applied Physics A*, *123*(8), p.563.
10. Tuan, N.H., Bac, L.H., Cuong, L.V., Van Thiet, D., Van Tam, T. and Dung, D.D., **2017**. Structural. Optical, and magnetic properties of lead-free ferroelectric $Bi_{0.5}K_{0.5}TiO_3$ solid solution with $BiFeO_3$ materials. *Journal of Electronic Materials, 46*(6), pp.3472–3478.
11. Zuo, X.Z., Yang, J., Yuan, B., Kan, X.C., Zu, L., Qin, Y.F., Zhu, X.B., Song, W.H. and Sun, Y.P., **2015**. Multiferroic properties of $Bi_{0.5}K_{0.5}TiO_3$–$BiFe_{1-x}Co_xO_3$ $(0 \leq x \leq 0.2)$ solid solution. *RSC Advances*, *5*(126), pp.104210–104215.
12. Zuo, R., Su, S., Wu, Y., Fu, J., Wang, M. and Li, L., **2008**. Influence of $A$-site nonstoichiometry on sintering, microstructure and electrical properties of $(Bi_{0.5}Na_{0.5})TiO_3$ ceramics. *Materials Chemistry and Physics*, *110*(2–3), pp.311–315.
13. Kimura, T., Fukuchi, E. and Tani, T., **2005**. Fabrication of textured bismuth sodium titanate using excess bismuth oxide. *Japanese Journal of Applied Physics*, *44*(11), pp.8055–8061.
14. Spreitzer, M., Valant, M. and Suvorov, D., **2007**. Sodium deficiency in $Na_{0.5}Bi_{0.5}TiO_3$. *Journal of Materials Chemistry*, *17*(2), pp.185–192.
15. Sung, Y.S., Kim, J.M., Cho, J.H., Song, T.K., Kim, M.H., Chong, H.H., Park, T.G., Do, D. and Kim, S.S., **2010**. Effects of Na nonstoichiometry in $(Bi_{0.5}Na_{0.5+x})TiO_3$ ceramics. *Applied Physics Letters*, *96*(2), Article ID: 022901.
16. Sung, Y.S., Kim, J.M., Cho, J.H., Song, T.K., Kim, M.H. and Park, T.G., **2010**. Roles of lattice distortion in $(1-x)(Bi_{0.5}Na_{0.5})TiO_3$-$xBaTiO_3$ ceramics. *Applied Physics Letters*, *96*(20), Article ID: 202901.
17. Quan, N.D., Huu Bac, L., Thiet, D.V., Hung, V.N. and Dung, D.D., **2014**. Current development in lead-free $Bi_{0.5}$(Na. K)$_{0.5}TiO_3$-based piezoelectric materials. *Advances in Materials Science and Engineering, 2014*, pp.1–13.
18. Co, N.D., Cuong, L.V., Tu, B.D., Thang, P.D., Dien, L.X., Hung, V.N. and Quan, N.D., **2019**. Effect of crystallization temperature on energy-storage density and efficiency of lead-free $Bi_{0.5}(Na_{0.8}K_{0.2})_{0.5}TiO_3$ thin films prepared by sol–gel method. *Journal of Science: Advanced Materials and Devices*, *4*(3), pp.370–375.
19. Quan, N.D., Toan, T.Q., Hung, V.N. and Nguyen, M.-D., **2019**. Influence of crystallization temperature on structural, ferroelectric and ferromagnetic properties of lead-free $Bi_{0.5}(Na_{0.8}K_{0.2})_{0.5}TiO_3$ multiferroic films. *Advances in Materials Science and Engineering*, *2019*, pp.1–10.
20. Quan, N.D., Toan, T.Q. and Hung, V.N., **2019**. Influence of crystallization time on energy-storage density and efficiency of lead-free $Bi_{0.5}(Na_{0.8}K_{0.2})_{0.5}TiO_3$ thin films. *Advances in Condensed Matter Physics*, *2019*, pp.1–8.
21. Quan, N.D., Hung, V.N. and Dung, D.D., **2017**. Influence of film thickness on ferroelectric properties and leakage current density in lead-free $Bi_{0.5}(Na_{0.80}$ $K_{0.20})_{0.5}TiO_3$ films. *Materials Research Express*, *4*(8), Article ID: 086401.

**22.** Quan, N.D., Quyet, N.V., Bac, L.H., Thiet, D.V., Hung, V.N. and Dung, D.D., **2015**. Structural, ferroelectric, optical properties of *A*-site-modified $Bi_{0.5}(Na_{0.78}K_{0.22})_{0.5}Ti_{0.97}Zr_{0.03}O_3$ lead-free piezoceramics. *Journal of Physics and Chemistry of Solids*, *77*, pp.62–67.

**23.** Quan, N.D., Hung, V.N., Kim, I.W. and Dung, D.D., **2016**. Bipolar electric field induced strain in Li substituted lead-free $Bi_{0.5}(Na_{0.82}K_{0.18})_{0.5}Ti_{0.95}Sn_{0.05}O_3$ piezoelectric ceramics. *Journal of Nanoscience and Nanotechnology*, *16*(8), pp.7978–7982.

**24.** Quan, N.D., Hung, V.N. and Dung, D.D., **2017**. Effect of Zr doping on structural and ferroelectric properties of lead-free $Bi_{0.5}(Na_{0.80}K_{0.20})_{0.5}TiO_3$ Films. *Journal of Electronic Materials*, *46*(10), pp.5814–5819.

**25.** Quan, N.D., Huong, C.T.T., Phuong, N.T.H., Hong, N.V., Hung, V.N. and Nguyen, M.-D., **2019**. Structural ferroelectric and energy-storage properties of lead-free Zr-doped $Bi_{0.5}(Na_{0.80}K_{0.20})_{0.5}TiO_3$ films. *Surface Review and Letters, 27*(1), Article ID: 1950082.

**26.** Hu, G.D., Fan, S.H., Yang, C.H. and Wu, W.B., **2008**. Low leakage current and enhanced ferroelectric properties of Ti and Zn codoped $BiFeO_3$ thin film. *Applied Physics Letters*, *92*(19), Article ID: 192905.

**27.** Zhang, Z., Wu, P., Lu, L. and Shu, C., **2008**. Defect and electronic structures of acceptor substituted lead titanate. *Applied Physics Letters*, *92*(11), Article ID: 112909.

**28.** Sung, Y.S., Kim, J.M., Cho, J.H., Song, T.K., Kim, M.H. and Park, T.G., **2011**. Effects of Bi nonstoichiometry in $(Bi_{0.5+x}Na)TiO_3$ ceramics. *Applied Physics Letters*, *98*(1), Article ID: 012902.

**29.** Pronin, I.P., Syrnikov, P.P., Isupov, V.A., Egorov, V.M. and Zaitseva, N.V., **2011**. Peculiarities of phase transitions in sodium–bismuth titanate. *Ferroelectrics*, *25*(1), pp.395–397.

Received: 26 November 2019. Accepted: 21 May 2020.